British Journal of Pharmacology (2006) 148, 786–794 © 2006 Nature Publishing Group All rights reserved 0007–1188/06 $30.00
www.nature.com/bjp

Phenobarbital increases monkey *in vivo* nicotine disposition and induces liver and brain CYP2B6 protein

[1]Anna M. Lee, [1]Sharon Miksys & *,[1]Rachel F. Tyndale

[1]Centre for Addiction and Mental Health, Department of Pharmacology, University of Toronto, Medical Sciences Building, Room 4336, 1 King's College Circle, Toronto, Ontario, Canada M5S 1A8

1 CYP2B6 is a drug-metabolizing enzyme expressed in the liver and brain that can metabolize bupropion (Zyban®, a smoking cessation drug), activate tobacco-smoke nitrosamines, and inactivate nicotine. Hepatic CYP2B6 is induced by phenobarbital and induction may affect *in vivo* nicotine disposition, while brain CYP2B6 induction may affect local levels of centrally acting substrates. We investigated the effect of chronic phenobarbital treatment on induction of *in vivo* nicotine disposition and CYP2B6 expression in the liver and brain of African Green (Vervet) monkeys.

2 Monkeys were split into two groups ($n=6$ each) and given oral saccharin daily for 22 days; one group was supplemented with 20 mg kg^{-1} phenobarbital. Monkeys were given a 0.1 mg kg^{-1} nicotine dose subcutaneously before and after treatment.

3 Phenobarbital treatment resulted in a significant, 56%, decrease ($P=0.04$) in the maximum nicotine plasma concentration and a 46% decrease ($P=0.003$) in the area under the concentration–time curve. Phenobarbital also increased hepatic CYP2B6 protein expression. In monkey brain, significant induction ($P<0.05$) of CYP2B6 protein levels was observed in all regions tested (caudate, putamen, hippocampus, cerebellum, brain stem and frontal cortex) ranging from 2-fold to 150-fold. CYP2B6 expression was induced in specific cells, such as frontal cortical pyramidal cells and thalamic neurons.

4 In conclusion, chronic phenobarbital treatment in monkeys resulted in increased *in vivo* nicotine disposition, and induced hepatic and brain CYP2B6 protein levels and cellular expression. This induction may alter the metabolism of CYP2B6 substrates including peripherally acting drugs such as cyclophosphamide and centrally acting drugs such as bupropion, ecstasy and phencyclidine.
British Journal of Pharmacology (2006) **148,** 786–794. doi:10.1038/sj.bjp.0706787;
published online 5 June 2006

Keywords: CYP2B6; monkey; nicotine; brain protein induction; phenobarbital; *in vivo* kinetics

Abbreviations: $AUC_{0-\infty}$, area under the curve extrapolated to infinity; AUC_t, area under the curve calculated to the last time measured; C_{max}, maximum concentration; CYP, cytochrome *P*450; CYP2A6, cytochrome *P*450 2A6; CYP2B1, cytochrome *P*450 2B1; CYP2B6, cytochrome *P*450 2B6; K_{el}, elimination constant; T_{max}, time of maximum concentration

Introduction

CYP2B6 is involved in the metabolism of a diverse variety of substances including clinical drugs such as bupropion (Zyban®, a smoking cessation drug) (Faucette *et al*., 2000), efavirenz (an anti-retroviral drug) (Ward *et al*., 2003; Rotger *et al*., 2005), cyclophosphamide (an anticancer drug) (Huang *et al*., 2000), drugs of abuse such as ecstasy (Kreth *et al*., 2000) and phencyclidine (Jushchyshyn *et al*., 2003), environmental toxins such as the tobacco-specific nitrosamine 4-methylnitrosamino-1-3-pyridyl-1-butanone (NNK) (Smith *et al*., 2003) and endogenous substances such as testosterone (Gervot *et al*., 1999) and serotonin (Fradette *et al*., 2004). Nicotine, the primary compound that maintains the addiction to cigarette smoking (Stolerman & Jarvis, 1995), is metabolized in the liver primarily by CYP2A6 to cotinine (Messina *et al*., 1997), which accounts for 80% of the metabolites of nicotine. Hepatic CYP2B6 can also metabolize nicotine to cotinine but with a lower affinity (Yamazaki *et al*., 1999; Dicke *et al*., 2005); it can also metabolize nicotine to the minor metabolite nornicotine (Yamanaka *et al*., 2005).

*Author for correspondence; E-mail: r.tyndale@utoronto.ca

The African Green monkey CYP2B6 (referred to as CYP2B6agm) protein (accession number GI 75053416, Q7M3F2) shares 91 and 75% amino-acid homology with human CYP2B6 and rat CYP2B1, respectively. We have previously investigated *in vitro* nicotine metabolism, hepatic CYP2A6agm and CYP2B6agm protein levels, and the effect of chronic phenobarbital treatment on these CYPs in African Green monkeys (Vervets, *Cercopithecus aethiops*) (Schoedel *et al*., 2003). In saline-treated monkeys, nicotine was metabolized *in vitro* by both CYP2A6agm and CYP2B6agm. Antibody inhibition studies and protein quantitation indicated that in saline-treated monkeys CYP2B6agm protein levels are 2.1-fold higher than CYP2A6agm, but are responsible for approximately 30% of nicotine metabolism *in vitro* (Schoedel *et al*., 2003). Phenobarbital is widely used in experimental studies as a protein inducer and is clinically used as a sedative and as an anti-epileptic. Phenobarbital treatment in monkeys resulted in an increase in total *in vitro* nicotine metabolism by 1.6-fold ($P=0.01$) (Schoedel *et al*., 2003). There was a 2.2-fold increase in CYP2B6agm-mediated *in vitro* nicotine metabolism ($P=0.001$) and a 6.6-fold increase in hepatic CYP2B6agm

protein levels ($P<0.001$), whereas neither CYP2A6agm-mediated nicotine metabolism ($P=0.90$) nor hepatic CYP2A6agm protein levels were different from controls (1.2-fold, $P=0.49$). Therefore, in phenobarbital-treated monkeys, the hepatic CYP2B6agm levels are approximately 12-fold higher than CYP2A6agm levels and are responsible for approximately 40% of nicotine metabolism *in vitro* (Schoedel *et al*., 2003). These data indicated that phenobarbital treatment did not significantly induce CYP2A6agm protein or activity but did increase both CYP2B6agm protein and CYP2B6agm-mediated *in vitro* nicotine metabolism in these monkeys. This raised the question of whether induction of hepatic CYP2B6agm protein and CYP2B6agm-mediated *in vitro* nicotine metabolism, without significant induction of CYP2A6agm, would affect *in vivo* nicotine disposition. Therefore, our first objective was to investigate the effect of phenobarbital treatment on *in vivo* nicotine disposition in these same African Green monkeys.

CYP2B6 is expressed in the liver but is also found in specific brain cells such as human cortical pyramidal cells and astrocytes (Miksys *et al*., 2003). Brain CYPs can be regulated differently from hepatic CYPs, for example rat brain CYP2B1 protein is induced by nicotine but hepatic CYP2B1 is not (Miksys *et al*., 2000). The induction of brain CYPs also occurs in specific cells, for example, rat brain CYP2B1 is induced in neurons of the frontal cortex, striatum and brainstem (Miksys *et al*., 2000). CYP induction in specific brain cells may result in a microenvironment where the metabolic activity differs from surrounding areas. This may alter the levels of therapeutic drugs (e.g. bupropion), drugs of abuse (e.g. nicotine), environmental toxins (e.g. NNK) and endogenous compounds (e.g. testosterone) in localized brain areas, but do not affect systemic drug or toxin levels. Phenobarbital induction of human hepatic CYP2B6 is well documented (Wang & Negishi, 2003); however, nothing is known about phenobarbital induction of human CYP2B6 in brain. Studies show that rat brain CYP2B1 protein (Anandatheerthavarada *et al*., 1992) and mRNA (Schilter & Omiecinski, 1993; Schilter *et al*., 2000) are induced after phenobarbital treatment.

We have previously investigated the induction of brain CYP2B6agm following chronic nicotine treatment in African Green monkeys (Lee *et al*., 2006). Nicotine increased CYP2B6agm expression in some brain regions such as the frontal cortex and hippocampus (Lee *et al*., 2006) while having no impact on hepatic CYP2B6agm (Schoedel *et al*., 2003). As phenobarbital is the classical hepatic CYP2B6 inducer, we were interested in whether it would also induce brain CYP2B6agm and if the induction would differ from that elicited by nicotine treatment. Therefore, our second objective was to determine if phenobarbital induced monkey brain CYP2B6agm and if so, in which brain regions and cells the induction occurred. The overall aim of this study was to investigate the effect of chronic phenobarbital treatment on *in vivo* nicotine disposition, and the cell-specific induction of brain CYP2B6 protein in monkeys.

Methods

Chemicals

All chemical reagents were obtained from standard commercial sources. Protein assay dye reagent was purchased from Bio-Rad Laboratories (Hercules, CA, U.S.A.). Pre-stained molecular weight protein markers were purchased from MBI Fermentas (Flamborough, ON, Canada). Nitrocellulose membrane was purchased from Pall Life Sciences (Pensacola, FL, U.S.A.). Human cDNA expressed CYP2B6 and polyclonal anti-rat CYP2B1 antibody were purchased from BD Gentest (Woburn, MA, U.S.A.). Polyclonal anti-CYP2B peptide antibody was purchased from Research Diagnostics Inc. (Concord, MA, U.S.A.). This antibody was produced from a synthetic peptide immunogen that is identical to the rat CYP2B1 and CYP2B2 amino-acid sequences (IDTYLLRMEKEK, Research Diagnositics Inc.), differs from the human CYP2B6 sequence by one amino acid (IDTYLL*H*MEKEK) and differs from the monkey CYP2B6agm sequence by two amino acids (ID*S*YLL*Q*MEKEK). Monoclonal anti-rat CYP2B1 antibody clone 4-7-1 for immunocytochemistry was a generous gift from Dr H.V. Gelboin (Goldfarb *et al*., 1993). Horseradish peroxidase-conjugated anti-rabbit secondary antibody was purchased from Chemicon International, Inc. (Temecula, CA, U.S.A.). Biotinylated anti-mouse secondary antibody, avidin-biotin complex with peroxidase kit and DAB were purchased from Vector Laboratories (Burlington, ON, Canada). Super-Signal West Pico and Femto chemiluminescence substrate was purchased from Pierce Chemical Company (Rockford, IL, U.S.A.). Autoradiographic film was purchased from Ultident (St Laurent, PQ, Canada).

Animals

Male African Green monkeys (*C. aethiops,* Vervet monkeys) were housed at Caribbean Primates Ltd (St Kitts). All monkeys ($n=12$) received oral saccharin daily for 22 days, while the phenobarbital-treated group ($n=6$) were supplemented with 20 mg kg^{-1} phenobarbital. Six monkeys per group was chosen based on a power estimate of a twofold difference in mean values between groups (as seen in *in vitro* nicotine metabolism), a type 1 error of 0.05 and 80% power to detect a difference. A 20 mg kg^{-1} oral dose was chosen based on phenobarbital induction of hepatic CYPs in other non-human primates (Jones *et al*., 1992; Bullock *et al*., 1995). The weights of the monkeys did not change as a result of the treatment. Monkeys were given standard rations of Purina monkey chow supplemented with fresh fruit and vegetables and drinking water was available *ad libitum*. One day before and 16 days after the start of phenobarbital treatment, a nicotine dose (0.1 mg kg^{-1}, subcutaneous (s.c.)) was administered; s.c. administration was used as this approximates the pharmacokinetics of the inhalation route usually used when smoking. The nicotine dose, 0.1 mg kg^{-1} s.c., was sufficiently low to avoid distress to the animals, but sufficient for analytical purposes. Blood was collected for pharmacokinetic analysis at time 0, 10, 20, 30, 60, 120, 240 and 360 min after injections under ketamine anaesthesia. On day 22, 6 h after morning phenobarbital or control treatments, all monkeys were killed under ketamine anaesthesia. Organs were immediately dissected, one half was flash frozen in liquid nitrogen and stored at -80°C until further use and the other half fixed in 4% paraformaldehyde. The experimental protocol was reviewed and approved by the Institutional Review Board of Behavioural Sciences Foundation and the University of Toronto Animal Care Committee. All procedures were conducted in

accordance with the guidelines of the Canadian Council on Animal Care.

Pharmacokinetics

Extraction and analysis of plasma nicotine concentrations from the pre- and post-treatment nicotine doses were performed as previously described (Xu *et al*., 2002; Sellers *et al*., 2003). The analytical sensitivity for nicotine was less than 0.5 ng ml^{-1} and the between- and within-day variation was less than 10%. Plasma was prepared by centrifugation of blood samples, then was frozen until analyzed for nicotine by HPLC. The internal standard was 5-methylnicotine and the limit of quantitation for nicotine was 0.5 ng ml^{-1}. Neither ketamine nor phenobarbital interfered with the analysis of nicotine and the internal standard. The results from the phenobarbital group are presented in this publication.

Immunocytochemistry

Immunocytochemical CYP2B6agm analysis was performed on frozen sections of fixed tissue as previously described (Lee *et al*., 2006). Briefly, the sections were washed with phosphate-buffered saline (PBS, 10 mM sodium phosphate buffer, 0.9% sodium chloride, pH 7.4) and incubated for 1 h in a blocking solution (PBS with 0.1% BSA, 0.01% Triton X-100 and 10% normal horse serum). The detection of monkey CYP2B6agm protein was assessed using the polyclonal anti-rat CYP2B1, the polyclonal anti-CYP2B peptide and the monoclonal anti-rat CYP2B1 antibodies. All three detected a similar staining pattern for CYP2B6agm in liver and brain tissue, increasing the probability that the detected protein is CYP2B6agm, and the monoclonal anti-rat CYP2B1 antibody was used for all subsequent immunocytochemistry assays. The brain and liver sections were incubated overnight at room temperature with monoclonal anti-rat CYP2B1 antibody diluted 1 : 1000. The tissue sections were washed, then reblocked for 30 min. The sections were then incubated for 1 h with biotinylated anti-mouse secondary antibody diluted 1 : 500. The antigen–antibody complex was visualized using the avidin–biotin complex followed by a reaction with 3,3′-diaminobenzidine and hydrogen peroxide. Immunocytochemical control sections were incubated without primary antibody.

Whole-membrane preparation and protein assay

Monkey tissues from brain regions were dissected by visual differentiation of the major brain regions based on brain atlases for the crab-eating macaque *(Macaca fascicularis)* (Martin & Bowden, 2000) and rhesus monkey *(Macaca mulatta)* (Snider & Lee, 1961). Whole membranes were prepared as previously described (Lee *et al*., 2006). Briefly, brain tissues were homogenized in 100 mM Tris, 0.1 mM EDTA, 0.1 mM DDT and 0.32 M sucrose (pH 7.4) then centrifuged at $3000 \times g$ for 10 min at 4°C. The supernatant was removed and the pellet centrifuged again for 10 min. The combined supernatant was then centrifuged at $110\,000 \times g$ for 60 min at 4°C and the pellet re-suspended in 100 mM Tris, 0.1 mM EDTA, 0.1 mM DDT, 1.15% w v^{-1} KCl and 20% v v^{-1} glycerol. The membranes were aliquoted and stored at −80°C. The protein content of brain membranes was assayed with the Bradford technique (Bradford, 1976) using a BioRad Protein Assay kit.

Immunoblotting

CYP2B6agm protein analysis was performed as previously described; no cross reactivity to CYPs, such as CYP1A1, 1A2, 2A6, 3A4, 2E1 and 2D6 was observed (Lee *et al*., 2006). Briefly, monkey brain membranes and cDNA expressed human CYP2B6 were serially diluted to generate standard curves and to establish a linear detection range for the assay. Membrane proteins (20–80 μg) were separated by SDS–PAGE using 8 or 10% separating gels and 4% stacking gels. To detect CYP2B6agm, the membranes were incubated for 1 h in a blocking solution of 2% w v^{-1} skim milk powder, 0.1% BSA, 0.1% Triton X-100 in Tris-buffered saline (TBS, 50 mM Tris, 150 mM NaCl, pH 7.4). The membranes were incubated for 1 h with polyclonal anti-CYP2B peptide antibody diluted 1 : 1000. Membranes were re-blocked with the same initial blocking solution for 45 min. To visualize CYP2B6agm, the membranes were incubated for 1 h with horseradish peroxidase conjugated anti-rabbit secondary antibody diluted 1 : 3000. CYP2B6agm proteins on immunoblots were detected using chemiluminescence and exposure to autoradiographic film for 1 to 5 min. MCID Elite imaging software (Imaging Research Inc., St Catherines, ON, Canada) was used to measure band densities from the films. The quantitation was performed by measuring the average optical density for a standard blot area that was identical for all the sample measurements on each blot. Baseline corrections were made by subtracting the density of the film background from the band density.

Statistical analysis

Pharmacokinetic variables from the pre- and post-treatment nicotine doses were calculated using SAS statistical software version 8.2. For each monkey, the mean nicotine-concentration time profile was derived and the area under the plasma concentration–time curves from time 0 to time t (AUC_t) was determined by the linear trapezoidal rule up to the last measured concentration. C_{max} was determined as the maximum of the mean concentration and T_{max} as the corresponding time where C_{max} occurred. The slope of the terminal phase of the plasma concentration–time curve was determined by fitting the data to a monoexponential equation. For the concentration–time profiles that clearly showed an exponential decay phase, the terminal rate constant, K_{el}, was determined from the slope, where the slope was obtained from the last 5 log concentration–time points for nicotine. Elimination half-life was calculated as 0.693 divided by K_{el}. The area under the curve from $AUC_{0-\infty}$ was determined by dividing the last measured concentration by the terminal rate constant K_{el}. The $AUC_{0-\infty}$ was the sum of the two partial AUCs. We hypothesize that chronic phenobarbital treatment will induce *in vivo* nicotine disposition and CYP2B6agm protein in monkeys. The within monkey differences in pre- and post-treatment kinetic variables were evaluated using a paired, one-tailed Student's t-test. A Bartlett's test was used to determine if the protein levels were normally distributed and they were

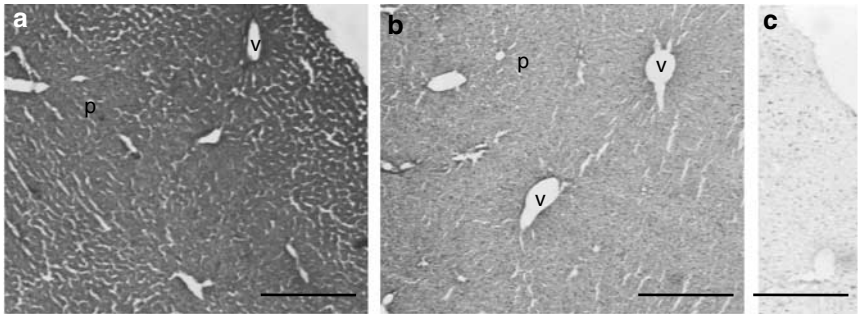

Figure 1 Phenobarbital-treated monkeys (a) had stronger hepatic CYP2B6agm immunoreactivity compared to control-treated monkeys (b). (c) Minimal immunoreactivity was seen in a section incubated without primary antibody. Hepatic central vein (v), portal vein (p), bars: 500 μm.

log normalized if required. Correlations between hepatic CYP2B6agm protein levels and pharmacokinetic variables were evaluated by a Pearson's correlation coefficient. The comparison of CYP2B6agm protein levels between the phenobarbital- and control-treated monkeys were evaluated using an unpaired one-tailed Student's *t*-test if the data was normally distributed and a one-tailed Mann–Whitney *U* test if the data was not normally distributed. Protein levels were expressed as mean $\pm$ s.d., which represents the average of at least four animals per group repeated three to eight times. Groups were deemed significantly different if $P \leqslant 0.05$.

Results

Hepatic CYP2B6agm expression was altered by phenobarbital treatment

Chronic phenobarbital treatment increased CYP2B6agm immunoreactivity in hepatic liver sections (Figure 1a and b) consistent with increased CYP2B6agm protein previously seen with immunoblotting (Schoedel *et al*., 2003). No immunoreactivity was seen in sections incubated without primary antibody (Figure 1c). CYP2B6agm expression in control- and phenobarbital-treated monkeys was uniform across the liver lobule.

Chronic phenobarbital treatment increased in vivo *nicotine disposition*

A graph of the plasma nicotine concentration–time curve pre- and post-phenobarbital treatment is shown in Figure 2a. Pre- and post-treatment pharmacokinetic parameters for the nicotine doses (0.1 mg kg^{-1}, s.c.) were calculated for each phenobarbital-treated monkey. A significant 56% reduction in the maximum plasma nicotine concentration (C_{max}) ($P = 0.04$) and a 46% decrease in the area under the concentration–time curve extrapolated to infinity ($AUC_{0-\infty}$) ($P = 0.003$, Table 1) were observed post-treatment compared to pretreatment. Post-phenobarbital treatment $AUC_{0-\infty}$ values were lower compared to the pre-phenobarbital treatment values for every monkey indicating a robust increase in nicotine clearance (Figure 2b). The time to maximum concentration, the elimination rate constant and the half-life were not substantially altered by phenobarbital treatment (Table 1).

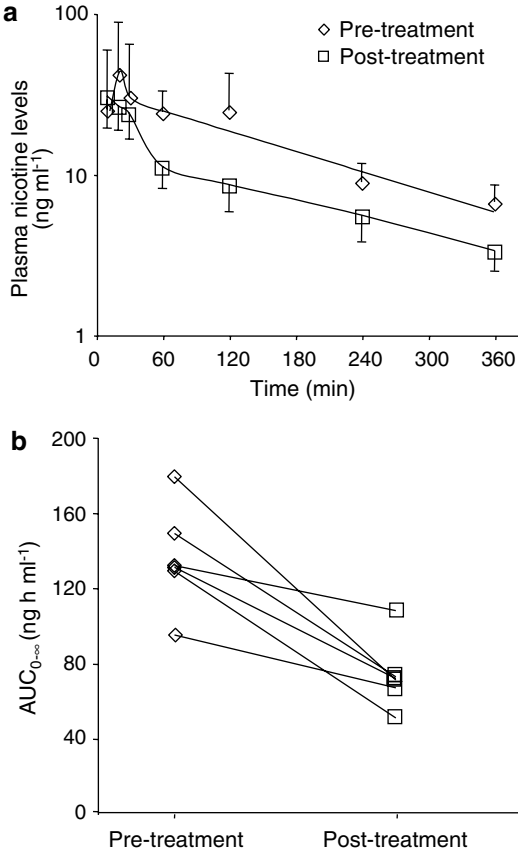

Figure 2 (a) The nicotine concentration–time curve after a 0.1 mg kg^{-1} s.c. nicotine injection pre- and post-phenobarbital treatment, expressed as the mean $\pm$ s.d. Each point represents the average nicotine concentration for all six monkeys. (b) Pre- and post-phenobarbital treatment $AUC_{0-\infty}$ for individual monkeys.

Chronic phenobarbital treatment induced brain CYP2B6agm protein

An immunoblotting assay was established to quantify brain CYP2B6agm protein. The linear range of the detection system was determined for each brain region using a serial dilution of phenobarbital-induced CYP2B6agm monkey brain membrane protein (Figure 3a). The amount of brain protein loaded for each region was chosen such that the control-treated monkey CYP2B6agm values were within the linear portion of the curve, above the limit of detection. Expressed human CYP2B6

Table 1 Pharmacokinetics for a 0.1 mg kg^{-1} nicotine dose in monkeys pre- and post-phenobarbital treatment ($n=6$)

Parameter	*Pretreatment*	*Post-treatment*
T_{max} (h)	0.61±0.69	0.25±0.14
C_{max} (ng ml^{-1})	73.6±38.9	32.1±13.6*
AUC_t (ng h ml^{-1})	100.8±24.4	57.2±19.9*
$AUC_{0-\infty}$ (ng h ml^{-1})[a]	135.8±27.5	73.7±18.7**
K_{el} (h^{-1})	0.29±0.20	0.20±0.10
Half-life (h)	3.4±2.1	3.2±1.0

[a]$AUC_{0-\infty}$ should be interpreted cautiously as the average proportions extrapolated for pretreatment was 25±15.1% and for post-treatment was 23±9.8% in contrast to the FDA standard of 20%.
Results are expressed mean±s.d., *$P<0.05$, **$P<0.01$.

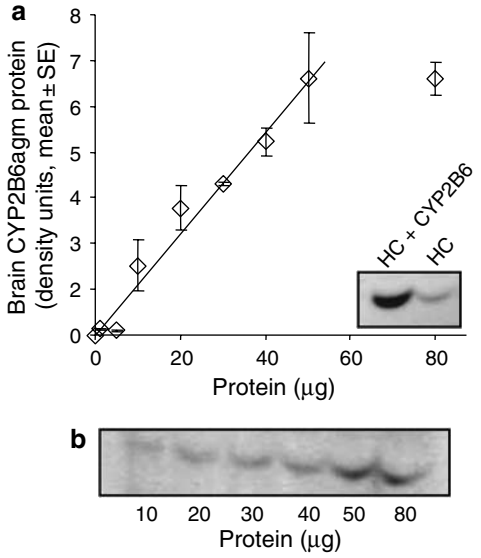

Figure 3 Brain CYP2B6agm immunoblot linearity was established using a dilution of brain membrane protein from phenobarbital-treated monkeys for each region assayed. (a) A representative standard curve used to determine linearity for the hippocampus, expressed as mean±s.e. The CYP2B6agm protein levels for the control group were detected at approximately 2 density units. Inset: The mobility of monkey brain CYP2B6agm was confirmed by adding 0.03 pmol expressed human CYP2B6 protein to 75 μg of phenobarbital-treated hippocampus (HC + CYP2B6) compared to 75 μg of phenobarbital-treated hippocampus only (HC). (b) Representative immunoblot of the phenobarbital-treated hippocampal CYP2B6agm dilution series. Migration increases slightly with increasing amounts of protein loaded. HC: Hippocampus.

was added to a sample of phenobarbital-treated monkey hippocampus to confirm the co-mobility of monkey brain CYP2B6agm (Figure 3a inset). A representative immunoblot of a hippocampal CYP2B6agm dilution curve is shown in Figure 3b.

For each brain region examined (caudate, putamen, hippocampus, cerebellum, brainstem and frontal cortex), the amount of CYP2B6agm protein was quantified in each control- and phenobarbital-treated monkey. For some brain regions in the phenobarbital-treated monkeys, the induced CYP2B6agm values were above the linear range of detection. To avoid underestimation of CYP2B6agm levels due to

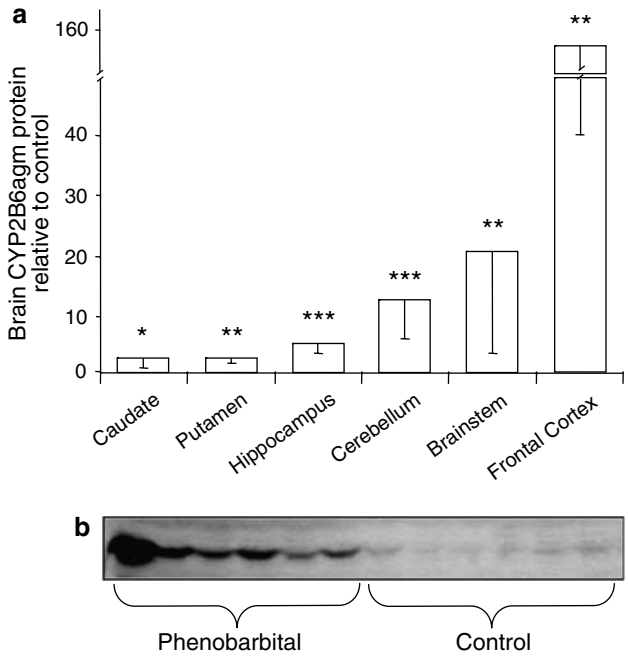

Figure 4 Phenobarbital induced CYP2B6agm in all brain regions assessed. (a) CYP2B6agm protein levels in brain regions of phenobarbital-treated monkeys relative to controls, *$P<0.05$, **$P<0.01$, ***$P<0.001$. (b) A representative immunoblot of hippocampal CYP2B6agm from control- and phenobarbital-treated monkeys (loaded at 75 μg). The leftmost phenobarbital-treated monkey hippocampus was omitted from analysis.

saturation of the assay, the CYP2B6agm levels were reassessed by reducing the amount of phenobarbital-treated brain membrane protein loaded onto the gels by the fold induction over control. Once within the linear range of detection, the CYP2B6agm levels for each phenobarbital-treated monkey were then adjusted according to the relative densities and the amount of protein loaded. One control-treated and one phenobarbital-treated monkey brainstem were unavailable for analysis. One control-treated monkey was omitted from cerebellar analysis and one phenobarbital-treated monkey was omitted from all brain region analyses because of extremely high CYP2B6agm protein levels, ranging from 10- to 90-fold higher than the average for the treatment group. For all brain regions examined chronic phenobarbital treatment significantly induced CYP2B6agm protein levels compared to control monkeys (Figure 4a). A wide range of inducibility was observed, ranging from approximately 2-fold in the caudate and putamen to 150-fold in the frontal cortex. The large standard deviation in each brain region (Figure 4a) is primarily due to the variation in CYP2B6agm levels among the phenobarbital-treated monkeys; less variation was observed among the control-treated monkeys. A representative immunoblot of hippocampal CYP2B6agm protein from control- and phenobarbital-treated monkeys is shown in Figure 4b.

Brain CYP2B6agm was induced in a cell-specific manner

Phenobarbital treatment induced CYP2B6agm immunoreactivity in many specific brain cells such as the thalamus (Figure 5a–d), the hippocampal CA2 region (Figure 5e–h), the frontal cortical pyramidal neurons (Figure 5i and j), the caudate

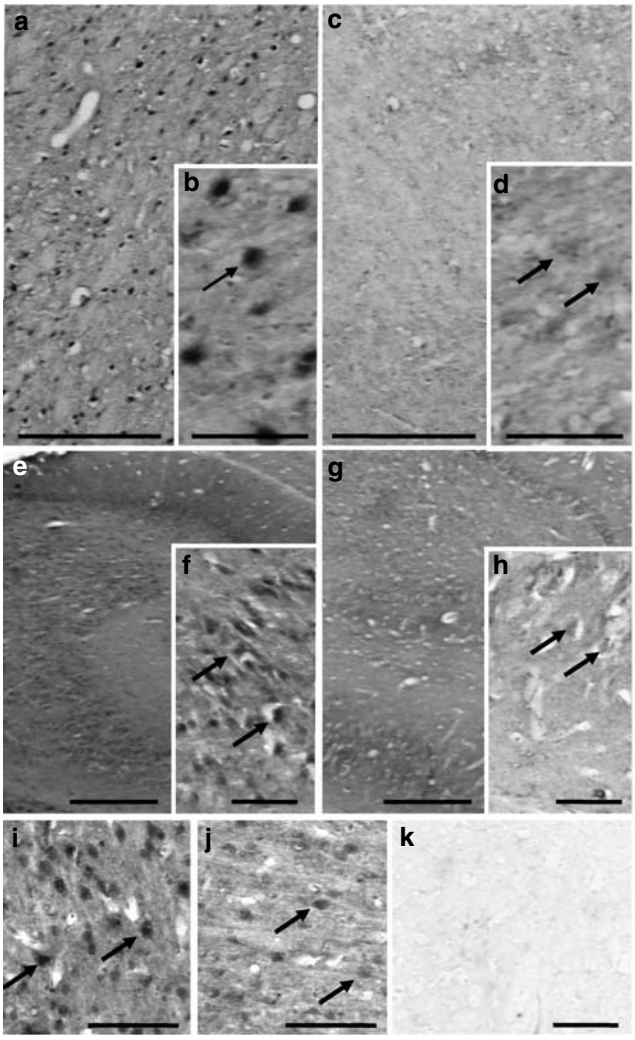

Figure 5 Phenobarbital treatment increased CYP2B6agm immunoreactivity in specific cells in the (a and b) thalamus, (e and f) hippocampal CA2 region and (i) frontal cortical pyramidal cells compared to their respective controls (c and d), (g and h) and (j). (k) No immunoreactivity was seen in a thalamic section incubated without primary antibody. Arrows indicate cells. a, c, e, g bars: 500 μm; b, d, f, h–k bars: 100 μm.

Table 2 Immunohistochemical assessment of brain CYP2B6agm protein expression in control- and phenobarbital-treated monkeys

Brain region	*Control*	*PB*
Frontal cortex		
Neuronal layer 1 astrocytes	***	***
Neuropil	**	***
Neuronal layer 2	**	****
Neuronal layer 3 and 5 (pyramidal cells)	***	****
White matter	—	—
White matter astrocytes	***	****
Cortex neuronal layer 5 (pyramidal cells)	***	****
Internal capsule	—	—
Caudate		
Body	*	*
Small neuronal cells	**	****
Putamen	*	**
Globus pallidus	*	*
Hippocampus		
Dentate gyrus molecular layer	**	**
Dentate gyrus granular layer	**	***
Dentate gyrus polymorphic layer	**	****
CA1 region	**	****
CA2 region	**	****
CA3 region	**	****
subiculum	**	****
Thalamic ventral lateral nucleus	**	****
Corticospinal and corticobulbar fibers	****	****
Optic tract	—	—
Lateral geniculate nucleus	****	****
Cerebellum		
Molecular layer	***	****
Purkinje cells	****	****
Granular layer	***	****
White matter	—	—
White matter astrocytes	****	****

Control levels have been previously reported in Lee *et al.* (2006). Levels should be interpreted as qualitative as they are derived from the semi-quantitative immunohistochemical assay.
****intense, ***strong, **moderate, *weak, — no staining.

and the cerebellum (Table 2). The induced immunoreactivity was expressed throughout the cell bodies. No CYP2B6agm immunoreactivity was detected in the internal capsule and white matter of either control- or phenobarbital-treated monkeys (Table 2). No immunoreactivity was seen in a section incubated without primary antibody (Figure 5k).

Discussion

Phenobarbital treatment significantly induced *in vivo* nicotine disposition in these African Green monkeys. Significant decreases in the maximum plasma nicotine concentration and $AUC_{0-\infty}$ were observed with no change in half-life or the elimination constant. These kinetic changes are also seen in rats; for example, phenobarbital-treated rats given intravenous nicotine have a trend for a twofold increase in nicotine clearance and a 40% decrease in the maximum plasma concentration (Foth *et al*., 1990). Increased hepatic metabolism in the presence of increased enzyme levels is also seen for other CYPs such as CYP2D6. Human subjects with extensive *CYP2D6* genotypes and metabolism showed a decrease in debrisoquine $AUC_{0-\infty}$ and an increase in C_{max} but no change in half-life compared to subjects with poor *CYP2D6* genotypes and metabolism, indicating that having more functional CYP2D6 increased debrisoquine hepatic metabolism after oral administration without altering subsequent systemic metabolism (Sloan *et al*., 1983; Dalen *et al*., 1999).

In humans, CYP2A6 is the main enzyme that metabolizes nicotine to cotinine with CYP2B6 as a secondary enzyme (Messina *et al*., 1997; Yamazaki *et al*., 1999). *In vitro*, human CYP2A6 has a higher affinity and a higher maximum velocity for nicotine metabolism compared to CYP2B6 (Yamazaki *et al*., 1999; Dicke *et al*., 2005). We have previously investigated *in vitro* nicotine metabolism and hepatic CYP2A6agm and CYP2B6agm protein levels in these African Green monkeys (Schoedel *et al*., 2003). Phenobarbital

treatment increased *in vitro* nicotine metabolism by 1.6-fold. There was no change in CYP2A6agm protein levels or CYP2A6agm-mediated nicotine metabolism, while there was a 6.6-fold increase in CYP2B6agm protein and a 2.2-fold increase in CYP2B6agm-mediated nicotine metabolism (Schoedel *et al*., 2003). Consistent with these observations, phenobarbital treatment in squirrel monkeys results in a 12-fold induction of hepatic CYP2B protein and a 3.3-fold induction of CYP2A protein (Ohmori *et al*., 1993). Phenobarbital also induces human hepatic CYP2B6 to a greater extent than CYP2A6 (Ohmori *et al*., 1993; Donato *et al*., 2000).

Among the phenobarbital-treated monkeys, a trend towards a correlation existed between *in vivo* $AUC_{0-\infty}$ ($r=-0.52$, $P=0.31$) and the elimination rate constant ($r=-0.64$, $P=0.18$) with the previously determined hepatic CYP2B6agm protein levels (Schoedel *et al*., 2003). Adding the hepatic CYP2A6agm protein levels (Schoedel *et al*., 2003) to the CYP2B6agm levels did not alter the significance of the correlations to the $AUC_{0-\infty}$ ($r=-0.46$, $P=0.50$) or the elimination rate constant ($r=-0.69$, $P=0.14$). This suggests that the main effect of phenobarbital treatment in African Green monkeys was to induce *in vivo* nicotine disposition, likely *via* the induction of CYP2B6agm protein. This conclusion is based on the lack of induction of CYP2A6agm protein or CYP2A6agm-mediated nicotine metabolism, the 6.6-fold increase in CYP2B6agm protein and 2.2-fold increase in CYP2B6agm-mediated *in vitro* nicotine metabolism, the 12-fold higher levels of CYP2B6agm than CYP2A6agm in phenobarbital-treated monkeys (Schoedel *et al*., 2003), and the lack of improvement in the correlations between hepatic CYP2B6agm protein levels and *in vivo* pharmacokinetic variables with the addition of CYP2A6agm levels.

It is possible, however, that other metabolic pathways are also involved in the induction of nicotine disposition. In humans, approximately 75–80% of nicotine is metabolized to cotinine, 3–5% is glucuronidated by uridine diphosphate-glucuronosyltransferase (UGT) 1A4 and 1A9 enzymes, 4–7% is converted to nicotine *N*′-oxide by flavin monooxygenase 3 (FMO3), 3% is metabolized to other minor products and 8–10% is excreted as nicotine in urine (for review see (Hukkanen *et al*., 2005)). Phenobarbital can induce both CYPs and UGTs (Soars *et al*., 2004) but not FMO3 (Chung *et al*., 1998). Although we have not investigated UGTs, it is likely that phenobarbital treatment in monkeys also induces nicotine glucuronidation; however, this is a very minor pathway (3–5%) and induction by phenobarbital is modest (Soars *et al*., 2004) suggesting a minor contribution to nicotine's clearance after phenobarbital induction.

Phenobarbital induces hepatic CYP2B6 *via* the constitutive androstane receptor (CAR) and increased CYP2B6 mRNA, although there is also evidence for the involvement of other nuclear receptors such as PXR (Goodwin *et al*., 2001; Pascussi *et al*., 2003). The mechanism underlying phenobarbital-induced brain CYP2B6 has not been investigated in monkeys. Phenobarbital can induce rat brain CYP2B1 mRNA (Schilter *et al*., 2000), thus it is likely that brain CYP2B6 protein induction occurs through a transcriptional mechanism similar to hepatic induction. The mechanism of CYP2A6 regulation by phenobarbital is unknown. We have previously shown that monkey hepatic CYP2A6 mRNA is not significantly induced by phenobarbital, although phenobarbital-induced CYP2A mRNA is seen in rodents (Donato *et al*., 2000).

Smokers aim to maintain a desired level of brain and plasma nicotine (McMorrow & Foxx, 1983) and altered nicotine disposition can result in altered smoking behaviour. Inhibition of nicotine metabolism with methoxalen (a CYP2A6 inhibitor) results in decreased nicotine clearance, higher nicotine plasma levels and decreased smoking behaviour (Sellers *et al*., 2000). Smokers with a *CYP2A6* gene duplication (two or more functional copies of *CYP2A6*) have faster removal of nicotine following smoking, increased breath carbon monoxide and increased smoking (Rao *et al*., 2000). Likewise, an increase in nicotine clearance, due to phenobarbital, may decrease nicotine plasma levels resulting in increased smoking behaviour.

Phenobarbital induction of hepatic CYP2B6 is well established but induction of primate brain CYP2B6 has not been previously investigated. We observed induction of monkey CYP2B6agm protein by immunoblotting in every brain region assessed. In contrast, nicotine treatment significantly induced CYP2B6agm in the frontal cortex (1.5-fold) with no induction in the other brain regions examined (Lee *et al*., 2006). However, in both nicotine- and phenobarbital-treated monkeys, the frontal cortex showed the highest levels of induction followed by the brainstem. The magnitude of induction by phenobarbital among the different brain regions was highly variable with the greatest induction (150-fold) considerably higher than the 6.6-fold increase in CYP2B6agm in monkey liver (Schoedel *et al*., 2003).

Phenobarbital treatment induced monkey brain CYP2B6agm protein expression in specific cells such as the neurons in the frontal cortex, thalamus, hippocampus and caudate. The cell-specific induction of CYP2B in brain is also seen in phenobarbital-treated rats given $80\,mg\,kg^{-1}$ phenobarbital intraperitoneally for 10 days (Upadhya *et al*., 2002). Phenobarbital-treated monkeys and rats have many similarities in the induction of CYP2B protein expression. Monkeys and rats (Upadhya *et al*., 2002) have high CYP2B immunoreactivity in cells such as the cortical neurons, thalamic neurons and pyramidal cells of the hippocampus following phenobarbital treatment. However, phenobarbital-treated monkeys also have strong immunoreactivity in the cerebellar molecular layer, whereas phenobarbital-treated rats do not (Upadhya *et al*., 2002). This difference in expression may be a result of a difference in the phenobarbital dose, route of administration or length of treatment.

CYP2B6 induction in brain may play a role in the central metabolism of nicotine. CYP2B6 protein is detectable in human brain tissue (Gervot *et al*., 1999; Miksys *et al*., 2003) but detectable levels of human brain CYP2A6 protein have not yet been reported. Phenobarbital has been shown to induce *in vitro* nicotine metabolism in rat brain tissues (Jacob *et al*., 1997), likely by induction of rat CYP2B1. The metabolism of other CYP2B substrates is also increased by phenobarbital treatment. For example, rats treated with phenobarbital have increased brain metabolism of benzyloxyresorufin-*O*-dealkylase (Dhawan *et al*., 1999) and pentoxyresorufin-*O*-dealkylase (Parmar *et al*., 1998; Dhawan *et al*., 1999). Human brain CYP2B6 may metabolize important centrally acting substrates such as nicotine, the antidepressant and smoking cessation drug bupropion and drugs of abuse such as ecstasy. Phenobarbital induction of CYP2B6 may increase the metabolism of these substrates in microenvironments within the brain.

In contrast to phenobarbital treatment in monkeys, nicotine treatment induced CYP2B6agm expression in fewer brain cell types, for example, no induction was seen in the cerebellar molecular layer, putamen and dentate gyrus polymorphic layer (Lee *et al*., 2006). However, the brain cell types that did show CYP2B6agm induction by nicotine treatment are also induced by phenobarbital treatment, for example the cortical neuronal layers, caudate neurons and hippocampal pyramidal cells. This indicates that phenobarbital and nicotine treatment induces brain CYP2B6agm in an overlapping pattern but that phenobarbital, by this route of administration and dose, may be a stronger inducer resulting in higher protein levels in more brain regions and cell types compared to nicotine.

There is little information on the mechanism of induction of brain CYPs in general. Brain CYP2B6agm induction by phenobarbital and nicotine may reflect similarities in the mechanism of induction. Phenobarbital induces human hepatic CYP2B6 *via* activation of the nuclear receptor CAR, which undergoes translocation to the nucleus to induce hepatic CYP2B6 transcription (Wang & Negishi, 2003). CAR mRNA has been detected at very low levels in the human brain (Lamba *et al*., 2004). The mechanism of brain CYP2B6 induction by phenobarbital is likely transcriptional as rat brain CYP2B1 mRNA is induced by phenobarbital (Schilter *et al*., 2000). However, while phenobarbital treatment induces both hepatic and brain CYP2B6agm, nicotine induces only brain CYP2B6agm (Lee *et al*., 2006) but not hepatic CYP2B6agm (Schoedel *et al*., 2003). The induction of brain CYP2B1 protein and mRNA by nicotine treatment, with no induction of hepatic CYP2B1, is also seen in rats (Miksys *et al*., 2000). This suggests that if phenobarbital and nicotine share a similar mechanism of induction in the brain, as indicated by the overlapping CYP2B6agm induction patterns, they may use an alternative transcription factor to CAR. It is also possible that CYP2B6agm induction in the brain involves alternative cellular mechanisms, different pathways of induction or different regulatory factors that result in variation in the degree of phenobarbital induction in different brain regions.

In summary, we have shown that chronic phenobarbital treatment induces *in vivo* nicotine disposition and hepatic and brain CYP2B6agm protein expression in African Green monkeys. This induction is likely *via* the induction of CYP2B6agm protein and CYP2B6agm-mediated nicotine metabolism as CYP2A6agm protein and activity are not induced (Schoedel *et al*., 2003). In addition to inducing hepatic CYP2B6agm, chronic phenobarbital treatment induced monkey brain CYP2B6agm protein levels in all brain regions examined and to very high levels (150-fold higher than control). CYP2B6agm expression was induced in specific brain cells such as the neurons in the frontal cortex, thalamus and hippocampus. Phenobarbital induced CYP2B6agm in similar brain cell types as seen with nicotine treatment (Lee *et al*., 2006) but also induced additional cell types and induction levels were substantially greater than with nicotine. This suggests that phenobarbital and nicotine may induce brain CYP2B6agm using similar mechanisms, with phenobarbital at these doses and route of administration being a stronger inducer. The induction of CYP2B6 in specific brain cells may affect the local metabolism of other centrally acting CYP2B6 substrates, such as bupropion and ecstasy, making the study of this in the future of great interest.

We thank Helma Nolte, Wenjiang Zhang and Lyndon Lacaya for excellent assistance. We are especially grateful to Drs Roberta Palmour and Edward Sellers for their expertise and assistance with interpretation. This work was supported by the Centre for Addiction and Mental Health and CIHR Grant MT14173. We are grateful for additional support from the CIHR Tobacco Use in Special Populations Fellowship to AML and a Canada Research Chair in Pharmacogenetics to RFT.

References

ANANDATHEERTHAVARADA, H.K., BOYD, M.R. & RAVINDRANATH, V. (1992). Characterization of a phenobarbital-inducible cytochrome P-450, NADPH-cytochrome P-450 reductase and reconstituted cytochrome P-450 mono-oxygenase system from rat brain. Evidence for constitutive presence in rat and human brain. *Biochem. J.,* **288,** 483–488.

BRADFORD, M.M. (1976). A rapid and sensitive method for the quantitation of microgram quantities of protein utilizing the principle of protein-dye binding. *Anal Biochem.,* **72,** 248–254.

BULLOCK, P., PEARCE, R., DRAPER, A., PODVAL, J., BRACKEN, W., VELTMAN, J., THOMAS, P. & PARKINSON, A. (1995). Induction of liver microsomal cytochrome P450 in cynomolgus monkeys. *Drug Metab. Dispos.,* **23,** 736–748.

CHUNG, W.G., ROH, H.K., KIM, H.M. & CHA, Y.N. (1998). Involvement of CYP3A1, 2B1, and 2E1 in C-8 hydroxylation and CYP 1A2 and flavin-containing monooxygenase in N-demethylation of caffeine; identified by using inducer treated rat liver microsomes that are characterized with testosterone metabolic patterns. *Chem. Biol. Interact.,* **113,** 1–14.

DALEN, P., DAHL, M.L., EICHELBAUM, M., BERTILSSON, L. & WILKINSON, G.R. (1999). Disposition of debrisoquine in Caucasians with different CYP2D6-genotypes including those with multiple genes. *Pharmacogenetics,* **9,** 697–706.

DHAWAN, A., PARMAR, D., DAYAL, M. & SETH, P.K. (1999). Cytochrome P450 (P450) isoenzyme specific dealkylation of alkoxyresorufins in rat brain microsomes. *Mol. Cell Biochem.,* **200,** 169–176.

DICKE, K.E., SKRLIN, S.M. & MURPHY, S.E. (2005). Nicotine and 4-(methylnitrosamino)-1-(3-pyridyl)-butanone metabolism by cytochrome p450 2b6. *Drug Metab. Dispos.,* **33,** 1760–1764.

DONATO, M.T., VIITALA, P., RODRIGUEZ-ANTONA, C., LINDFORS, A., CASTELL, J.V., RAUNIO, H., GOMEZ-LECHON, M.J. & PELKONEN, O. (2000). CYP2A5/CYP2A6 expression in mouse and human hepatocytes treated with various *in vivo* inducers. *Drug Metab. Dispos.,* **28,** 1321–1326.

FAUCETTE, S.R., HAWKE, R.L., LECLUYSE, E.L., SHORD, S.S., YAN, B., LAETHEM, R.M. & LINDLEY, C.M. (2000). Validation of bupropion hydroxylation as a selective marker of human cytochrome P450 2B6 catalytic activity. *Drug Metab. Dispos.,* **28,** 1222–1230.

FOTH, H., WALTHER, U.I. & KAHL, G.F. (1990). Increased hepatic nicotine elimination after phenobarbital induction in the conscious rat. *Toxicol. Appl. Pharmacol.,* **105,** 382–392.

FRADETTE, C., YAMAGUCHI, N. & DU SOUICH, P. (2004). 5-Hydroxytryptamine is biotransformed by CYP2C9, 2C19 and 2B6 to hydroxylamine, which is converted into nitric oxide. *Br. J. Pharmacol.,* **141,** 407–414.

GERVOT, L., ROCHAT, B., GAUTIER, J.C., BOHNENSTENGEL, F., KROEMER, H., DE BERARDINIS, V., MARTIN, H., BEAUNE, P. & DE WAZIERS, I. (1999). Human CYP2B6: expression, inducibility and catalytic activities. *Pharmacogenetics,* **9,** 295–306.

GOLDFARB, I., KORZEKWA, K., KRAUSZ, K.W., GONZALEZ, F. & GELBOIN, H.V. (1993). Cross-reactivity of thirteen monoclonal antibodies with ten vaccinia cDNA expressed rat, mouse and human cytochrome P450s. *Biochem. Pharmacol.,* **46,** 787–790.

GOODWIN, B., MOORE, L.B., STOLTZ, C.M., MCKEE, D.D. & KLIEWER, S.A. (2001). Regulation of the human CYP2B6 gene by the nuclear pregnane X receptor. *Mol. Pharmacol.,* **60,** 427–431.

HUANG, Z., ROY, P. & WAXMAN, D.J. (2000). Role of human liver microsomal CYP3A4 and CYP2B6 in catalyzing N-dechloroethylation of cyclophosphamide and ifosfamide. *Biochem. Pharmacol.,* **59,** 961–972.

HUKKANEN, J., JACOB III, P. & BENOWITZ, N.L. (2005). Metabolism and disposition kinetics of nicotine. *Pharmacol. Rev.,* **57,** 79–115.

JACOB III, P., ULGEN, M. & GORROD, J.W. (1997). Metabolism of (−)-(S)-nicotine by guinea pig and rat brain: identification of cotinine. *Eur. J. Drug Metab. Pharmacokinet.,* **22,** 391–394.

JONES, C.R., GUENGERICH, F.P., RICE, J.M. & LUBET, R.A. (1992). Induction of various cytochromes CYP2B, CYP2C and CYP3A by phenobarbitone in non-human primates. *Pharmacogenetics,* **2,** 160–172.

JUSHCHYSHYN, M.I., KENT, U.M. & HOLLENBERG, P.F. (2003). The mechanism-based inactivation of human cytochrome P450 2B6 by phencyclidine. *Drug Metab. Dispos.,* **31,** 46–52.

KRETH, K., KOVAR, K., SCHWAB, M. & ZANGER, U.M. (2000). Identification of the human cytochromes P450 involved in the oxidative metabolism of 'Ecstasy'-related designer drugs. *Biochem. Pharmacol.,* **59,** 1563–1571.

LAMBA, J.K., LAMBA, V., YASUDA, K., LIN, Y.S., ASSEM, M., THOMPSON, E., STROM, S. & SCHUETZ, E.G. (2004). Expression of CAR splice variants in human tissues and their functional consequences. *J. Pharmacol. Exp. Ther.,* **311,** 811–821.

LEE, A.M., MIKSYS, S., PALMOUR, R. & TYNDALE, R.F. (2006). CYP2B6 is expressed in African Green monkey brain and is induced by chronic nicotine treatment. *Neuropharmacology,* **50,** 441–450.

MARTIN, R.F. & BOWDEN, D.M. (2000). *Primate Brain Maps: Structure of the macaque brain: A Laboratory Guide with Original Brain Sections*. Amsterdam, Oxford: Elsevier (Printed atlas and electronic templates for data and schematics by Richard F. Martin and Douglas M. Bowden; software by John Wu, Mark F. Dubach and Joan E. Robertson).

MCMORROW, M.J. & FOXX, R.M. (1983). Nicotine's role in smoking: an analysis of nicotine regulation. *Psychol. Bull.,* **93,** 302–327.

MESSINA, E.S., TYNDALE, R.F. & SELLERS, E.M. (1997). A major role for CYP2A6 in nicotine C-oxidation by human liver microsomes. *J. Pharmacol. Exp. Ther.,* **282,** 1608–1614.

MIKSYS, S., HOFFMANN, E. & TYNDALE, R.F. (2000). Regional and cellular induction of nicotine-metabolizing CYP2B1 in rat brain by chronic nicotine treatment. *Biochem. Pharmacol.,* **59,** 1501–1511.

MIKSYS, S., LERMAN, C., SHIELDS, P.G., MASH, D.C. & TYNDALE, R.F. (2003). Smoking, alcoholism and genetic polymorphisms alter CYP2B6 levels in human brain. *Neuropharmacology,* **45,** 122–132.

OHMORI, S., HORIE, T., GUENGERICH, F.P., KIUCHI, M. & KITADA, M. (1993). Purification and characterization of two forms of hepatic microsomal cytochrome P450 from untreated cynomolgus monkeys. *Arch. Biochem. Biophys.,* **305,** 405–413.

PARMAR, D., DHAWAN, A. & SETH, P.K. (1998). Evidence for O-dealkylation of 7-pentoxyresorufin by cytochrome P450 2B1/2B2 isoenzymes in brain. *Mol. Cell Biochem.,* **189,** 201–205.

PASCUSSI, J.M., GERBAL-CHALOIN, S., DROCOURT, L., MAUREL, P. & VILAREM, M.J. (2003). The expression of CYP2B6, CYP2C9 and CYP3A4 genes: a tangle of networks of nuclear and steroid receptors. *Biochim. Biophys. Acta.,* **1619,** 243–253.

RAO, Y., HOFFMANN, E., ZIA, M., BODIN, L., ZEMAN, M., SELLERS, E.M. & TYNDALE, R.F. (2000). Duplications and defects in the CYP2A6 gene: identification, genotyping, and *in vivo* effects on smoking. *Mol. Pharmacol.,* **58,** 747–755.

ROTGER, M., COLOMBO, S., FURRER, H., BLEIBER, G., BUCLIN, T., LEE, B.L., KEISER, O., BIOLLAZ, J., DECOSTERD, L. & TELENTI, A. (2005). Influence of CYP2B6 polymorphism on plasma and intracellular concentrations and toxicity of efavirenz and nevirapine in HIV-infected patients. *Pharmacogenet. Genomics,* **15,** 1–5.

SCHILTER, B., ANDERSEN, M.R., ACHARYA, C. & OMIECINSKI, C.J. (2000). Activation of cytochrome P450 gene expression in the rat brain by phenobarbital-like inducers. *J. Pharmacol. Exp. Ther.,* **294,** 916–922.

SCHILTER, B. & OMIECINSKI, C.J. (1993). Regional distribution and expression modulation of cytochrome P-450 and epoxide hydrolase mRNAs in the rat brain. *Mol. Pharmacol.,* **44,** 990–996.

SCHOEDEL, K.A., SELLERS, E.M., PALMOUR, R. & TYNDALE, R.F. (2003). Down-regulation of hepatic nicotine metabolism and a CYP2A6-like enzyme in African green monkeys after long-term nicotine administration. *Mol. Pharmacol.,* **63,** 96–104.

SELLERS, E.M., KAPLAN, H.L. & TYNDALE, R.F. (2000). Inhibition of cytochrome P450 2A6 increases nicotine's oral bioavailability and decreases smoking. *Clin. Pharmacol. Ther.,* **68,** 35–43.

SELLERS, E.M., RAMAMOORTHY, Y., ZEMAN, M.V., DJORDJEVIC, M.V. & TYNDALE, R.F. (2003). The effect of methoxsalen on nicotine and 4-(methylnitrosamino)-1-(3-pyridyl)-1-butanone (NNK) metabolism *in vivo*. *Nicotine Tob. Res.,* **5,** 891–899.

SLOAN, T.P., LANCASTER, R., SHAH, R.R., IDLE, J.R. & SMITH, R.L. (1983). Genetically determined oxidation capacity and the disposition of debrisoquine. *Br. J. Clin. Pharmacol.,* **15,** 443–450.

SMITH, G.B., BEND, J.R., BEDARD, L.L., REID, K.R., PETSIKAS, D. & MASSEY, T.E. (2003). Biotransformation of 4-(methylnitrosamino)-1-(3-pyridyl)-1-butanone (NNK) in peripheral human lung microsomes. *Drug Metab. Dispos.,* **31,** 1134–1141.

SNIDER, R.S. & LEE, J.C. (1961). A sterotaxic atlas of the monkey brain (*Macaca mulatta*). Chicago, University Press.

SOARS, M.G., PETULLO, D.M., ECKSTEIN, J.A., KASPER, S.C. & WRIGHTON, S.A. (2004). An assessment of udp-glucuronosyltransferase induction using primary human hepatocytes. *Drug Metab. Dispos.,* **32,** 140–148.

STOLERMAN, I.P. & JARVIS, M.J. (1995). The scientific case that nicotine is addictive. *Psychopharmacology (Berlin),* **117,** 2–10; discussion 14–20.

UPADHYA, S.C., CHINTA, S.J., PAI, H.V., BOYD, M.R. & RAVINDRANATH, V. (2002). Toxicological consequences of differential regulation of cytochrome p450 isoforms in rat brain regions by phenobarbital. *Arch. Biochem. Biophys.,* **399,** 56–65.

WANG, H. & NEGISHI, M. (2003). Transcriptional regulation of cytochrome p450 2B genes by nuclear receptors. *Curr. Drug Metab.,* **4,** 515–525.

WARD, B.A., GORSKI, J.C., JONES, D.R., HALL, S.D., FLOCKHART, D.A. & DESTA, Z. (2003). The cytochrome P450 2B6 (CYP2B6) is the main catalyst of efavirenz primary and secondary metabolism: implication for HIV/AIDS therapy and utility of efavirenz as a substrate marker of CYP2B6 catalytic activity. *J. Pharmacol. Exp. Ther.,* **306,** 287–300.

XU, C., RAO, Y.S., XU, B., HOFFMANN, E., JONES, J., SELLERS, E.M. & TYNDALE, R.F. (2002). An *in vivo* pilot study characterizing the new CYP2A6*7, *8, and *10 alleles. *Biochem. Biophys. Res. Commun.,* **290,** 318–324.

YAMANAKA, H., NAKAJIMA, M., FUKAMI, T., SAKAI, H., NAKAMURA, A., KATOH, M., TAKAMIYA, M., AOKI, Y. & YOKOI, T. (2005). CYP2A6 and CYP2B6 are involved in nornicotine formation from nicotine in humans: interindividual differences in these contributions. *Drug Metab. Dispos,* **33,** 1811–1818.

YAMAZAKI, H., INOUE, K., HASHIMOTO, M. & SHIMADA, T. (1999). Roles of CYP2A6 and CYP2B6 in nicotine C-oxidation by human liver microsomes. *Arch. Toxicol.,* **73,** 65–70.

(Received December 22, 2005
Revised March 27, 2006
Accepted April 20, 2006
Published online 5 June 2006)